Techno-economic and environmental analyses of a novel, sustainable process for production of liquid fuels using helium heat transfer

Authors:

Leila Hoseinzade, Thomas A Adams II

Date Submitted: 2019-06-25

Keywords: Negative emissions, Fischer-Tropsch Synthesis, Carbonless heat, Dimethyl Ether, Gasification, Methane Reforming, Biomass

Abstract:

In this paper, several new processes are proposed which co-generate electricity and liquid fuels (such as diesel, gasoline, or dimethyl ether) from biomass, natural gas and heat from a high temperature gas-cooled reactor. This carbonless heat provides the required energy to drive an endothermic steam methane reforming process, which yields H2-rich syngas (H2/CO > 6) with lower greenhouse gas emissions than traditional steam methane reforming processes. Since downstream Fischer-Tropsch, methanol, or dimethyl ether synthesis processes require an H2/CO ratio of around 2, biomass gasification is integrated into the process. Biomass-derived syngas is sufficiently H2-lean such that blending it with the steam methane reforming derived syngas yields a syngas of the appropriate H2/CO ratio of around 2. In a prior work, we also demonstrated that integrating carbonless heat with combined steam and CO2 reforming of methane is a promising option to produce a syngas with proper H2/CO ratio for Fischer-Tropsch and methanol/dimethyl ether applications. In this study, we presented another novel design called gas-nuclear-to-liquids process which can be applied for liquid fuel production without needing H2/CO adjustment. Chemical process simulations of several candidate processes were developed, which used the rigorous multi-scale, two-dimensional, heterogeneous models for the carbonless-heat-powered steam methane reforming and mixed reforming of methane processes developed in prior works in gPROMS. In addition, 1D process models within Aspen Plus were also used (Aspen Plus simulation and gPROMS models are provided to the reader). The performance of the presented systems was compared with a biomass-gas-to-liquids plant where heat from gasification drives the steam methane reforming instead of the high temperature gas-cooled reactor. Techno-economic analyses and greenhouse gas life cycle analyses of each case were completed to investigate the economic and environmental impacts of the proposed processes. Optional carbon capture and sequestration technology is also considered. The analysis demonstrates that carbonless heat integration leads to thermal efficiencies of up to 55% (high heating value based) as well as suitable profits in the right market conditions. It is also found that net negative life cycle greenhouse gas emissions of the final products can be achieved owing to use of biomass, carbonless heat, and carbon capture and sequestration. Even without carbon capture and sequestration, the life cycle greenhouse gas emissions of the proposed process are 25–57% lower than traditional natural gas-to-dimethyl ether and coal-to- dimethyl ether processes.

Record Type: Preprint

Submitted To: LAPSE (Living Archive for Process Systems Engineering)

Citation (overall record, always the latest version):	LAPSE:2019.0609
Citation (this specific file, latest version):	LAPSE:2019.0609-1
Citation (this specific file, this version):	LAPSE:2019.0609-1v1

DOI of Published Version: https://doi.org/10.1016/j.apenergy.2018.12.006

Techno-economic and environmental analyses of a novel, sustainable process for production of liquid fuels using helium heat transfer

Leila Hoseinzade, Thomas A. Adams II*

Department of Chemical Engineering, McMaster University, 1280 Main St W,

Hamilton, Ontario, L8S 4L8, Canada

tadams@mcmaster.ca

Abstract

In this paper, several new processes are proposed which co-generate electricity and liquid fuels (such as diesel, gasoline, or dimethyl ether (DME)) from biomass, natural gas and heat from a high temperature gas-cooled reactor (HTGR). This carbonless heat provides the required energy to drive an endothermic steam methane reforming (SMR) process, which yields H_2-rich syngas (H_2/CO>6) with lower greenhouse gas (GHG) emissions than traditional SMR processes. Since downstream Fischer-Tropsch, methanol, or dimethyl ether synthesis is processes require an H_2/CO ratio of around 2, biomass gasification is integrated into the process. Biomass-derived syngas is sufficiently H_2-lean such that blending it with the SMR-derived syngas yields a syngas of the appropriate H_2/CO ratio of around 2. Chemical process simulations of several candidate processes were developed, which used a rigorous multi-scale, two-dimensional, heterogeneous model for the carbonless-heat-powered SMR reactor developed in a prior work in gPROMS. In addition, 1D process models within Aspen Plus were also used (Aspen Plus simulation files are provided to the reader). The performance of the presented system was compared with a biomass-gas-to-liquids (BGTL) plant where heat from gasification drives the SMR instead of the HTGR. Techno-economic analyses and GHG life cycle analyses of each case were completed to investigate the economic and environmental impacts of the proposed processes. Optional carbon capture and sequestration (CCS) technology is also considered. The analysis demonstrates that

carbonless heat integration leads to thermal efficiencies of up to 55 HHV% as well as suitable profits in the right market conditions. It is also found that net negative life cycle GHG emissions of the final products can be achieved owing to use of biomass, carbonless heat, and CCS. Even without CCS, the life cycle GHG emissions of the proposed process is 25-57% lower than traditional natural gas-to-DME and coal-to-DME processes.

Keywords: Biomass, Natural gas, Carbonless Heat, Dimethyl ether, Fischer-Tropsch Synthesis, Negative emissions.

1. Introduction

The gas-to-liquids (GTL) process can produce liquid fuels from natural gas by reforming natural gas into syngas (a mixture of H_2 and CO) and then converting syngas to synthetic diesel and gasoline using the Fischer-Tropsch (FT) synthesis route [1]. GTL processes can be more economical than traditional petroleum-based plants when natural gas prices are low [1]. The coal-to-liquid (CTL) process is another alternative which produces syngas from the gasification of coal before converting the syngas to liquid fuels via the FT process [2]. This process is also economic when the price of coal is low [2]. However, they both have significantly negative environmental impacts [3] that are even worse than traditional petroleum refining [4]. Carbon capture and sequestration (CCS) technologies can be used to reduce the greenhouse gas (GHG) emissions of GTL and CTL plants, but unfortunately it causes the energy efficiency of the plants to drop remarkably [5]. However, GHG emissions can be reduced from GTL or CTL plants without the use of CCS by integrating them with other processes in a synergistic way that results in efficiency improvements [6, 7].

Polygeneration was introduced to efficiently utilize resources such as coal and gas [8]. Adams et al. defined polygeneration as a thermochemical process which simultaneously co-generates at least two products; one of the products is electricity and the other one is a fuel or a chemical [9]. Polygeneration systems are known by their improved efficiency [10] and flexibility comparing to the standalone processes which produce only one product [11]. In most polygeneration systems, syngas is the main route to generate fuels, chemicals or electricity. To produce syngas in polygeneration processes, possible feedstocks and energy sources could include coal, natural gas, biomass, petroleum coke, nuclear energy, wind energy, steel refining off-gases, and so on, either

alone or in combination. Based on Adams et al. [9], the products of the polygeneration plants include a wide range such as electricity, FT liquids (gasoline and diesel), alcohols, olefins, dimethyl ether (DME), H_2, syngas, heat, cooling and so on.

Adams et al. [12, 13] and Khojasteh et al. [14] have found that processes which combine natural gas (or coal) with other fuels can harness certain synergies that provide significant benefits. In the studies by Adams et al. [12, 13], natural gas reforming and coal gasification are integrated to poly-generate fuels, chemicals and electricity. It was demonstrated that by integrating the processes, the efficiency and profitability of the plant are significantly improved compared to the coal only and gas only processes.

In the study by Khojasteh et al. [14], an advanced type of nuclear reactor called a Modular Helium Reactor (MHR) is used as the source of heat and electricity, and coal and natural gas are employed as the carbon source. Heat from the high-temperature MHR is used to provide energy to the endothermic SMR reaction. This process is called coal-gas-and-nuclear-to-liquids (CGNTL), which is environmentally and economically superior to coal-to-liquids (CTL), coal-and-gas-to-liquids (CGTL), and other processes in most market conditions. However, even if all CO_2 emissions from the CGNTL plant can be captured, avoided, or eliminated, the CO_2 emissions from combusting the fuels downstream cannot be prevented. Furthermore, in some areas, the use of coal is either not permitted or not of interest due either to a lack of access, lack of political support, or other concerns. This is the case for the region considered in this study (the province of Ontario, Canada), which has eliminated coal from its power grid by public policy [15].

Scott et al. [16] recently presented an alternative to this process which used biomass instead of coal, called the biomass-gas-and-nuclear-to-liquids process (BGNTL). Unlike the process of Khojasteh et al. [14], the BGNTL process of Scott et al. used a Generation IV CanDu Supercritical Water Reactor which was not integrated with the SMR. Instead, heat from this reactor was used as the energy source of a copper-chloride (CuCl) cycle, which produces hydrogen that is blended into biomass-derived syngas for upgrading. This reduces the use of either biomass or gas combustion for heat production needs, thus lowering the amount of CO_2 that is generated during the process and increasing its carbon efficiency. However, it was found that comparing to a base case version that does not use nuclear energy (a biomass-gas-to-liquids

process, or BGTL) at the same capacity, it was not economical to use nuclear energy in this way [16]. One of the key reasons for this is that the CuCl process is not particularly efficient at producing hydrogen, and the amount of fossil fuel consumption for hydrogen production that is avoided using this technique is limited.

Therefore, in this study, we propose a novel alternative to the BGNTL/CuCl process of Scott et al. [16] which avoids this limitation by using a high temperature gas-cooled reactor (HTGR) instead of a CanDU reactor. Our proposed process, which we call the BGTNL/HTGR process, uses heat at >800°C from the HTGR to provide energy for the endothermic SMR reaction. This allows a greater proportion of nuclear energy to be used in the process (thus displacing a greater amount of fossil fuel) and permits hydrogen production at greater efficiency. Our proposed process is similar in approach to the CGNTL process of Khojestah et al. [14], except for three important factors: (1) our process is designed for biomass instead of coal; (2) our process is designed to work with HGTRs with coolant temperatures in the 800-950°C range, while the process of Khojestah et al. is designed for very high temperature MHR reactors operating around 1200°C; and (3) our process uses a rigorous multi-scale model for the integrated HTGR/SMR system, with much more realistic properties. This is the primary novelty of the work. The use of biomass in our process is less efficient and less economical than coal, but can yield significant environmental benefits. The lower temperature HGTR used in our process has fewer practical limitations than the 1200°C MHR, but it also creates additional process challenges since it reduces the efficacy of the SMR reaction. For example, the SMR reactor designs are fundamentally different, since the helium-heated SMR in the present work is driven primarily by convection, while the helium-heated SMR in Khojestah et al. is driven primarily by radiative heat transfer.

In this paper the economic and environmental impacts of the proposed BGNTL/HGTR process is compared with a “best known” base case BGTL process with integrated biomass gasification and SMR. Other BGTL, GTL, or BTL processes were not considered for comparison since previous studies found that they were not as efficient or environmentally friendly than the base case used in our work [14].

The proposed BGNTL process is shown in Figure 1. In this process, biomass is gasified with steam and oxygen into syngas and wastes such as CO_2. The produced syngas contains a low

amount of H_2 (molar H_2/CO ratio of about 0.75); However, a higher H_2 concentration (H_2/CO≈2) is required for the downstream use in either FT liquids synthesis or DME synthesis processes. To meet this need, natural gas and steam are converted into the hydrogen rich syngas through the steam reforming reaction ($CH_4 + H_2O \rightarrow CO + 3H_2$). This syngas has a high H_2 content (H_2/CO>6), and it can be mixed with the biomass-derived syngas to produce syngas with a balanced H_2 content (H_2/CO≈2) required for the downstream processes. CO_2 produced in the process can be captured and sequestered, providing a process which produces near zero direct CO_2 emissions and uses enough biomass to offset the most of GHG emissions from the use of the fuels downstream (e.g. gasoline combustion).

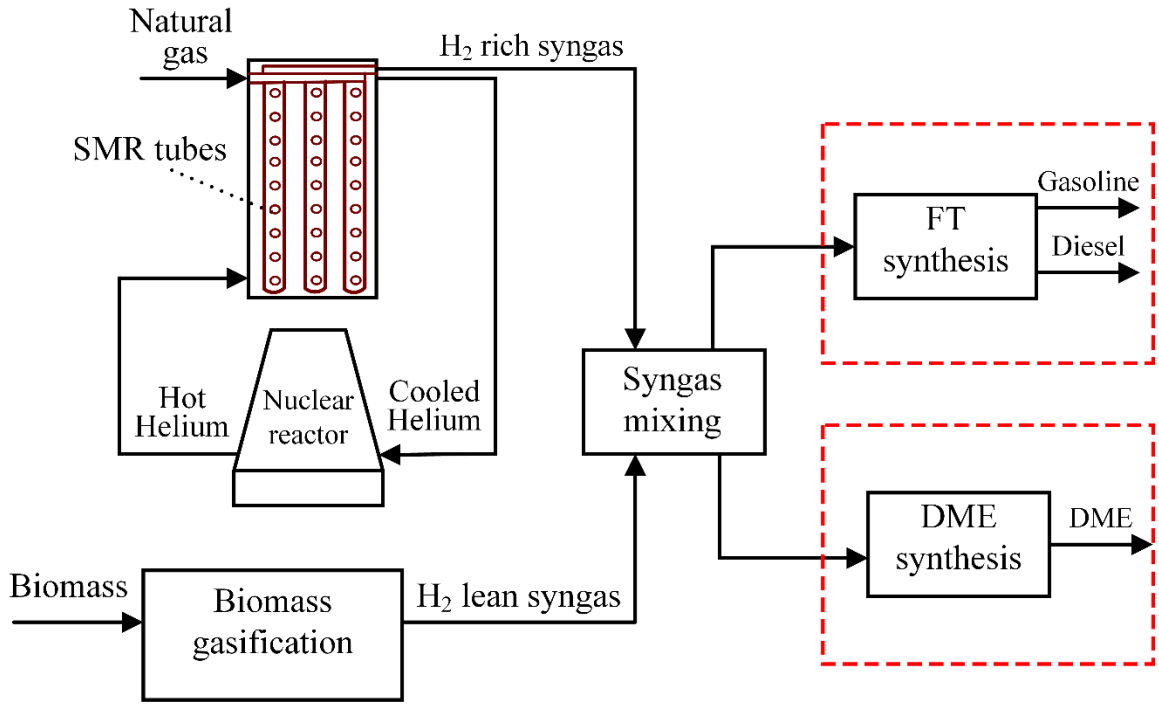

Figure 1. General overview of the BGNTL system superstructure.

The concept of using the heat from a HTGR to power SMR is not new. Several studies by the Research Center Julich and SIEMENS-INTERATOM research groups in Germany [17, 18, 19] and the Japan Atomic Energy Research Center [20] have examined the feasibility and safety of the concept when helium is used as a high-temperature transfer medium which carries heat from the HTGR to the SMR reactor. The studies included the demonstration of pilot scale versions of the helium-heated SMR unit. Hoseinzade et al. [21, 22] later developed a rigorous model for the helium-heated SMR reactor based on first principles and validated it against the design data of

the prior work. We used this model in the present work in order to design a helium-heated SMR reactor suitable for use in a BGNTL system and predict the operating conditions pertinent to the system (such as temperature profiles, methane conversions and yields, steam and heat consumption, etc.). Then, we designed a BGNTL system which incorporates this reactor, and performed systems-level techno-economic and life cycle GHG emission analyses in order to evaluate the efficiency of the approach from a business, environmental, and technical perspective. Aspen Plus models were used to aid in these analysis, which have been made available to the public through LAPSE: the Living Archive for Process Systems Engineering at PSEcommunity.org.

2. Methodology

A recent literature review found that in the large majority of cases, creating multiple kinds of fuels in a polygeneration process is generally less economic than producing a single kind of fuel unless there are particular business reasons for needing to multiple kinds of fuels [9]. We found this to be true for the proposed BGNTL system as well [23]. Therefore, in this work, we considered BGNTL variants which produced either FT liquids or DME as products, but not both.

Eight different cases were studied in this work, each at steady state conditions. The cases are BGTL/FT to produce FT liquids (gasoline and diesel), BGTL/DME to produce DME with and without CCS, BGNTL/FT to produce FT liquids and BGTNTL/DME to produce DME with and without CCS. BGTL cases do not include a nuclear component but BGNTL cases contain a HTGR. Each case was sized to have 1070 MW_{HHV} thermal input including woody biomass, natural gas, and nuclear heat (in the BGNTL cases). It should be noted that nuclear heat amount does not represent the nuclear reactor size, it is the amount of heat delivered by the helium coolant to drive the SMR process. A combination of different software packages including Aspen Plus V10, ProMax, gPROMS, and MATLAB were used to simulate these processes. However, most of the process sections except CO_2 removal and integrated steam reforming systems were modeled using Aspen Plus. The Peng-Robinson equation of state with the Boston-Mathias modification (PR-BM) physical property package was used for most of the Aspen Plus simulations which is consistent with a prior work [12]. PSRK method was applied for the CO_2/water mixture at high pressures. In a prior study [24], the PSRK method was found to match experimental data for the property prediction of CO_2/water mixture at high pressures very well.

For the MeOH/DME separation NRTL-RK was used [12] and NBS/NRC tables were used for the water-only streams. ProMax software was applied to model the CO_2 removal processes due to its superior physical property models (TSWEET) for this acid gas removal systems. The model of the CO_2 removal process was developed by Adams et al. [25]. The integrated RSC/SMR system and integrated HTGR/SMR processes were modeled in the gPROMS software package.

2.1 Steam Reforming Sections for BGTL Cases

Figure 2 shows the integrated RSC/SMR unit used in the BGTL cases. The model for this system, which was developed by Ghouse et al. [26], is based on first principles and validated in that work using experimental data. The model is a rigorous, multi-scale, and two dimensional and accounts for both the bulk gas phase changes as well as spatial differences within the catalyst particles. The produced syngas in the gasifier is H_2-lean (H_2/CO ~1) and has the temperature as high as 1300°C. In order to cool down the gasifier derived syngas, it is integrated with a steam methane reforming process which is highly endothermic. Ghouse et al. [26] found that for safe operation of the integrated RSC/SMR process, the co-current configuration should be applied which assures the tube wall temperature remains below the structural integrity limit.

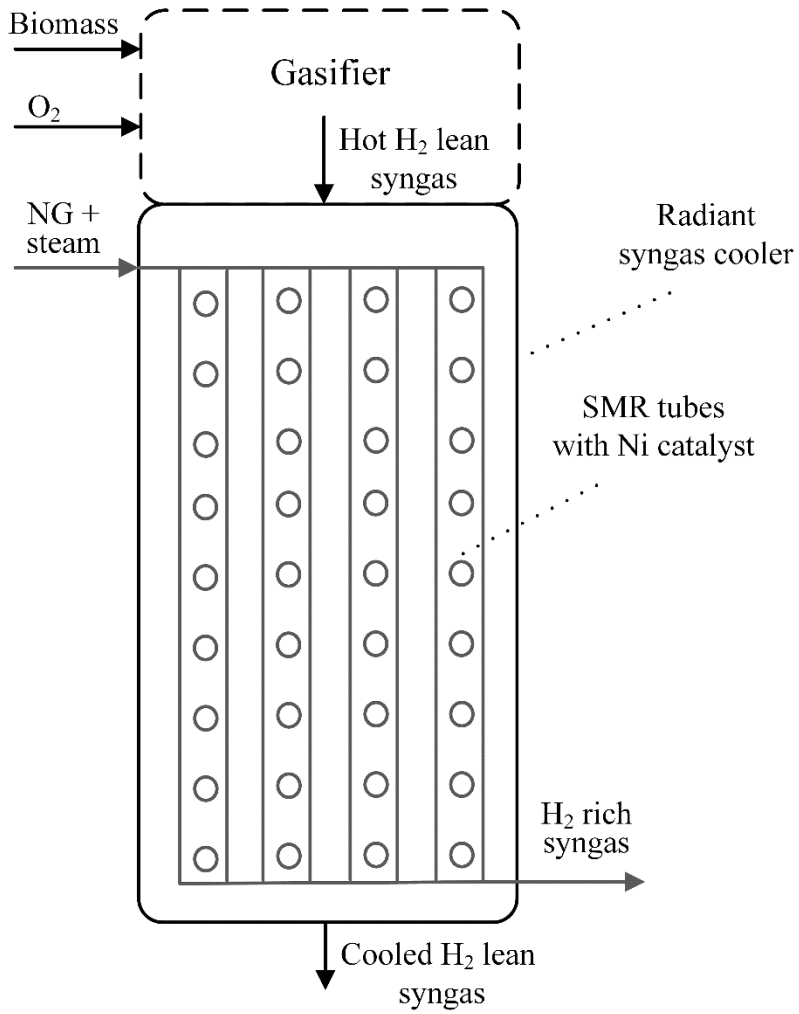

Figure 2. Integrated RSC/SMR system [26].

As Figure 2 shows, syngas from the gasifier flows through the radiant syngas cooler and transfers heat to the SMR tube walls mostly by the radiative heat transfer mechanism. In the tube side, methane and steam are mixed, receive heat from the tube walls, and then are converted to hydrogen rich syngas. The optimal design of the integrated system was presented in follow-up study by Ghouse et al. [27] and it was applied in the BGTL process design. The RSC/SMR system used in this study contains 200 SMR tubes with an outer tube diameter of 10 (cm), tube length of 20 (m), gasifier inner diameter of 4.572 (m) and catalyst particle diameter of 1.6 (cm). More details on the integrated RSC/SMR model can be find in the study by Ghouse et al. [26].

2.2 Steam Reforming Sections for BGTNL Cases

The BGNTL cases use an integrated HTGR/SMR approach shown in Figure 3. The model for this section was developed in gPROMS by Hoseinzade et al. [21] in a prior work, and is also rigorous and based on first principles. The model was validated in that work using design data from two pilot plants. As indicated in the figure, high temperature helium from an HTGR or an intermediate heat exchanger flows in the shell side of a shell and tube heat exchanger. The helium temperature at the shell entrance is 950°C, thus convection is the dominant heat transfer mechanism. Some disc type fins are installed in the outer surface of the SMR tubes to increase the flow turbulence and the heat transfer coefficient. Each SMR tube contains an inner tube (which is not packed with catalyst) to recover the heat of the produced high temperature syngas and increase the methane conversion. The designed system includes 199 SMR tubes with an outer diameter of 12 (cm), tube length of 14 (m), inner tube diameter of 6 (cm), refractory inner diameter of 2.7 (m), and a catalyst particle diameter of 1.2 (cm). Some of these design parameters where chosen to match the plant design by SIEMENS-INTERATOM, while others such as the catalyst particle size or inner tube diameter were determined through a manual optimization procedure (a course-mesh sampling approach).

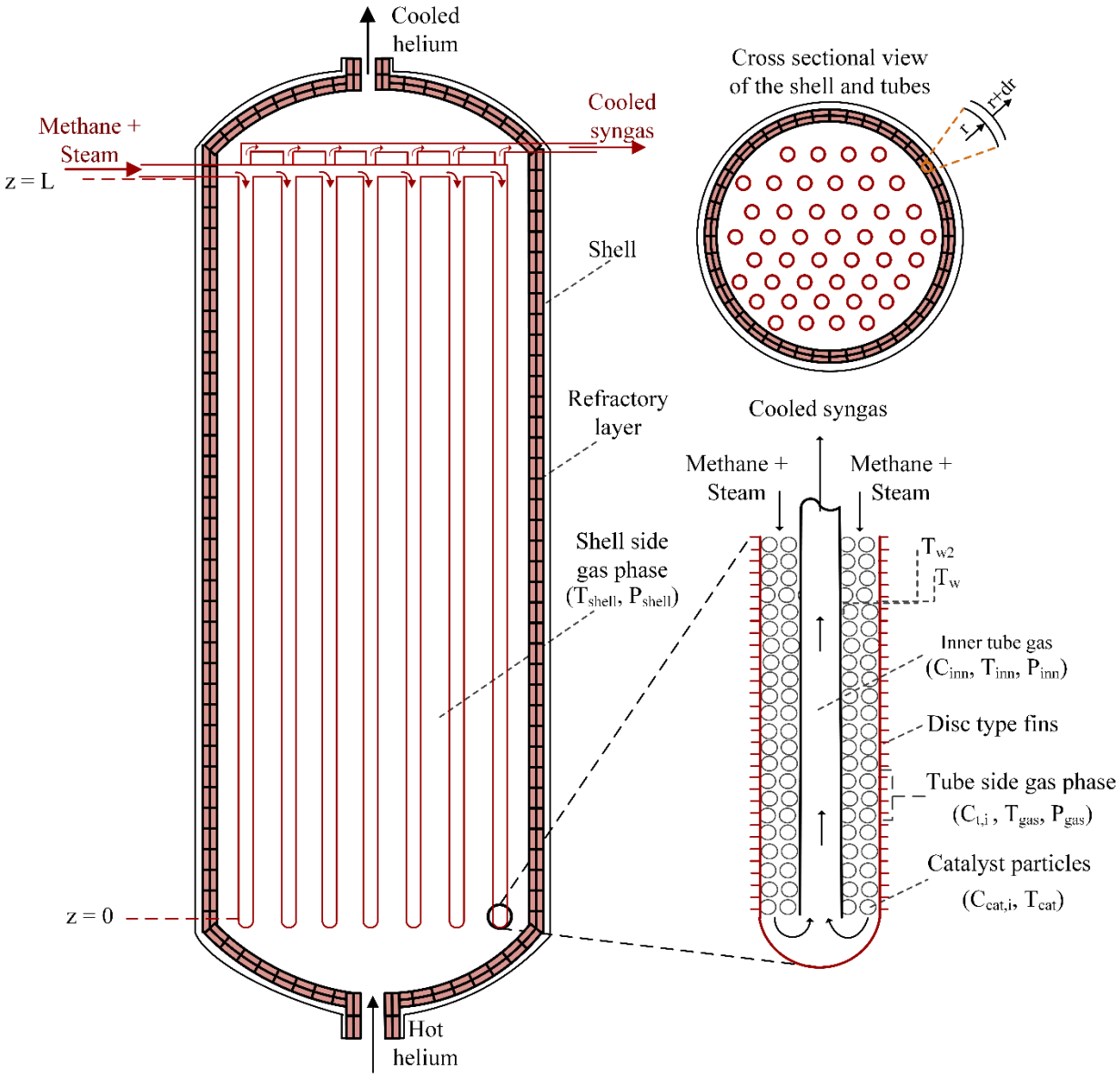

Figure 3. Integrated HTGR/SMR system super structure. This figure is reprinted from the study by Hoseinzade et al. [21].

2.3 Biomass Gasification and Biomass-Derived Syngas Upgrading

Much of the remaining portions of the Aspen Plus process models of the BGTL and BGNTL processes were based on individual model components which were each developed and optimized in our prior works, including gasification [28], water gas shift [29], CO_2 removal [25], FT synthesis [12], and DME synthesis [30]. Therefore, most of the sections of the process are described briefly in this study and detailed descriptions of those sections can be found in the latter references. The biomass (Ontario cedar wood chips) and natural gas properties used in this study are given in Table 1. It is assumed that the average molecular weight of ash is 0.06515

(kg/mol), the mole fraction of Fe_2O_3 in ash is 2.613% [31], and natural gas is available at 30°C and 30 bar.

Table 1. Properties of wood and natural gas used in this study.

Wood: proximate analysis – as received (wt%) [32]					
Fixed carbon	Volatile matter	Ash	Moisture	HHV (kJ/kg)	LHV (kJ/kg)
58.16	39.94	1.90	8.00	19804.82	18790.00
Wood: ultimate analysis (dry wt%) [32]					
Carbon	Hydrogen	Nitrogen	Sulfur	Oxygen	Chlorine
48.620	5.991	0.478	0.005	43.006	0.209
Natural gas mole fraction (%) [14]					
Methane	Ethane	Propane	n-Butane	CO_2	N_2
93.9	3.2	0.7	0.4	1.0	0.8

Figure 4 and 5 show the schematic of the BGTL/FT, BGTL/DME, BGNTL/FT, and BGNTL/DME processes. The processes start with biomass crushing and feeding to an entrained-flow gasifier. It is assumed that 0.02 kWe is required to crush 1 kWth (HHV based) of wood [33]. Woody biomass, high purity oxygen from the air separation unit (ASU), steam, and CO_2 are fed into the gasifier to produce syngas. The biomass gasification model contains three stages: biomass decomposition, gasification, and cooling. The model was originally developed by Field et al. [34] for coal gasification was adapted and modified for biomass gasification [16]. The produced high temperature syngas in the gasifier transfers its heat via a radiant syngas cooler to either the integrated steam reforming process in the BGTL cases or the steam generator in heat recovery steam generator (HRSG) section in BGNTL cases.

Then, the biomass-derived syngas is desulfurized before sending to the syngas mixing section. First, it is sent to a hydrolysis reactor where COS reacts with water, generating H_2S, which is easier to remove than COS from syngas, making downstream sulfur removal more cost efficient [12]. The H_2S amount in the raw syngas is low (in the range of 50 ppm) for wood gasification process, thus it is economic to remove it using the LO-CAT process [35]. The LO-CAT system uses a catalyst to oxidize the H_2S into solid sulfur [36]. This system is not modeled in Aspen Plus but it is accounted in the economic analysis. It should be noted that the ASU unit was not

modeled in Aspen Plus either, however, it was considered in the economic and energy analysis. It is assumed that 1 MWe is required to produce 1 kg/s oxygen at 1 bar and 0°C [37].

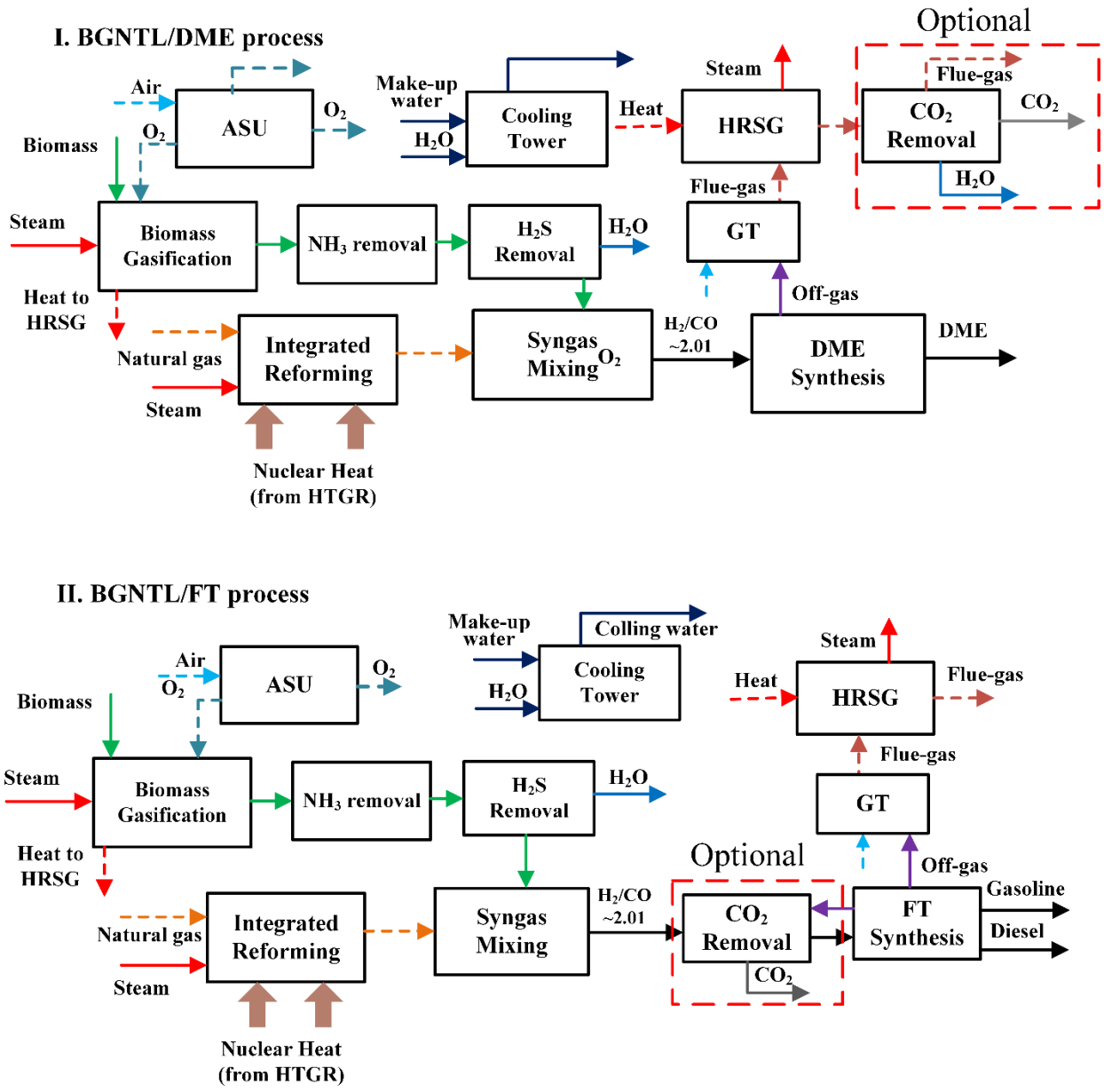

Figure 4. Schematic of BGNTL/DME and BGNTL/FT processes. (GT = Power generation using a gas combustion turbine)

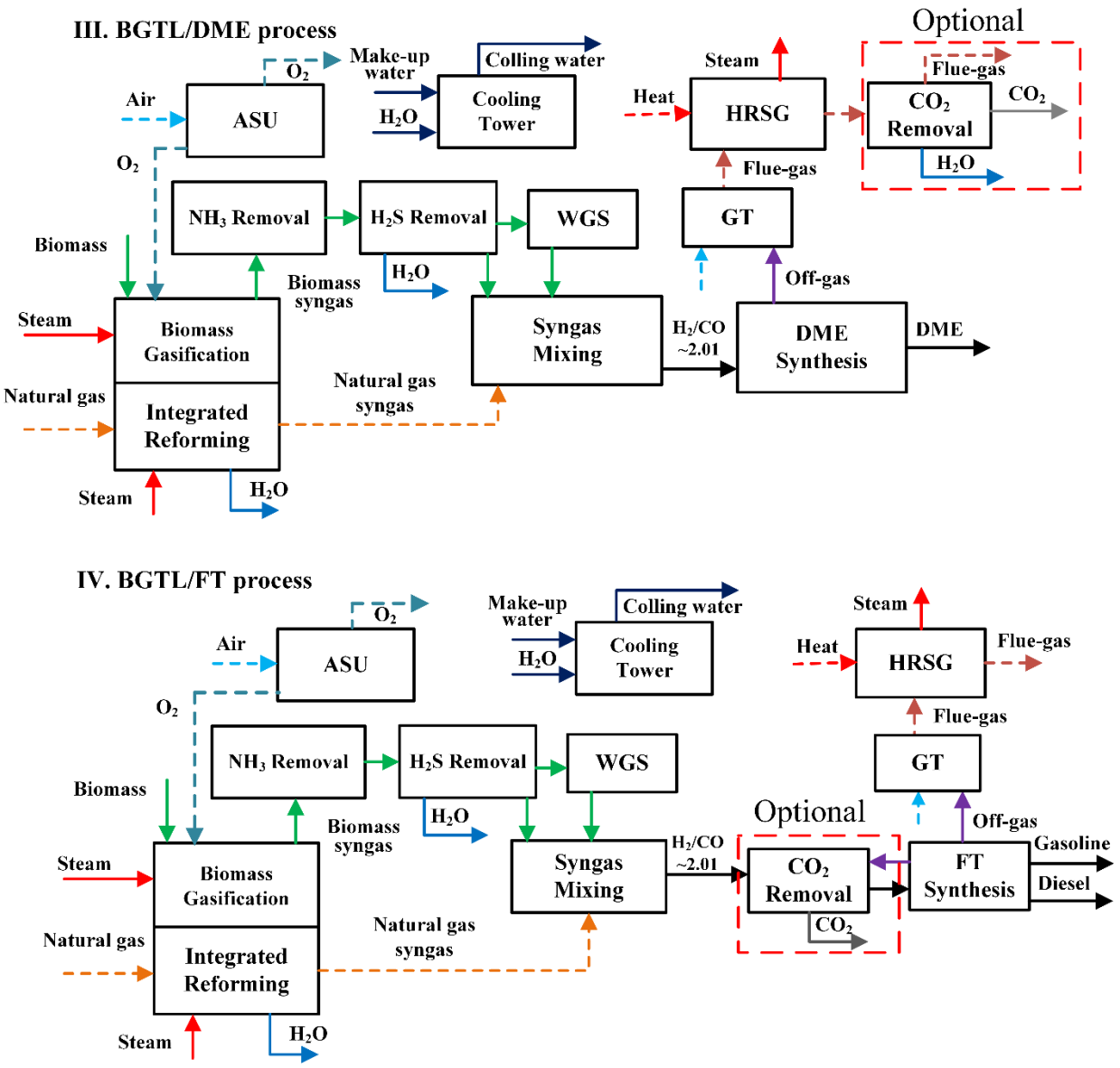

Figure 5. Schematic of the BGTL/DME and BGTL/FT processes.

In the BGTL processes, desulfurized syngas was upgraded to obtain the desired H_2/CO ratio for the Fischer-Tropsch (FT) and methanol/DME processes using the water-gas shift (WGS) reaction. The WGS section was modeled using series of three adiabatic-equilibrium reactors in Aspen Plus to benefit from the fast kinetics at higher temperature in the first two reactors and high conversion at low temperature in the last reactor [29].

2.4 Natural Gas Reforming

In the BGTL cases the integrated reforming section includes a pre-reformer and an integrated RSC/SMR system. The pre-reformer converts the C_2-C_4 hydrocarbons to syngas and is adiabatic. Methane is then reformed to H_2-rich syngas in the integrated RSC/SMR system. The latter design is similar to the integrated coal gasification and SMR system which was presented and modeled by Ghouse et al. [26]. The pre-reformer and reformer were modeled in Aspen Plus assuming chemical equilibrium.

Figure 6 shows a more detailed schematic for this system as modelled in Aspen Plus. As shown in the figure, a pre-reformer converts ethane, propane and butane to syngas first, then output gases are split into two streams of the equal molar flow rate and fed to two integrated HTGR/SMRs operating in parallel. The reason for using two HTGR/SMRs is to prevent high pressure drop in the SMR tubes. If only one reactor is used at this particular process capacity, the pressure drop exceeds 20 bar (as predicted by the rigorous model in gPROMS). The integrated HTGR/SMR system was modeled in Aspen Plus with a combination of a reactor model (specifically REQUIL with specified extents of conversions of the SMR and WGS reactions based on the gPROMS results) and a heater. The heater determines the outlet gas temperature. The results of the gPROMS model were directly entered into the Aspen Plus model of the integrated HTGR/SMR system.

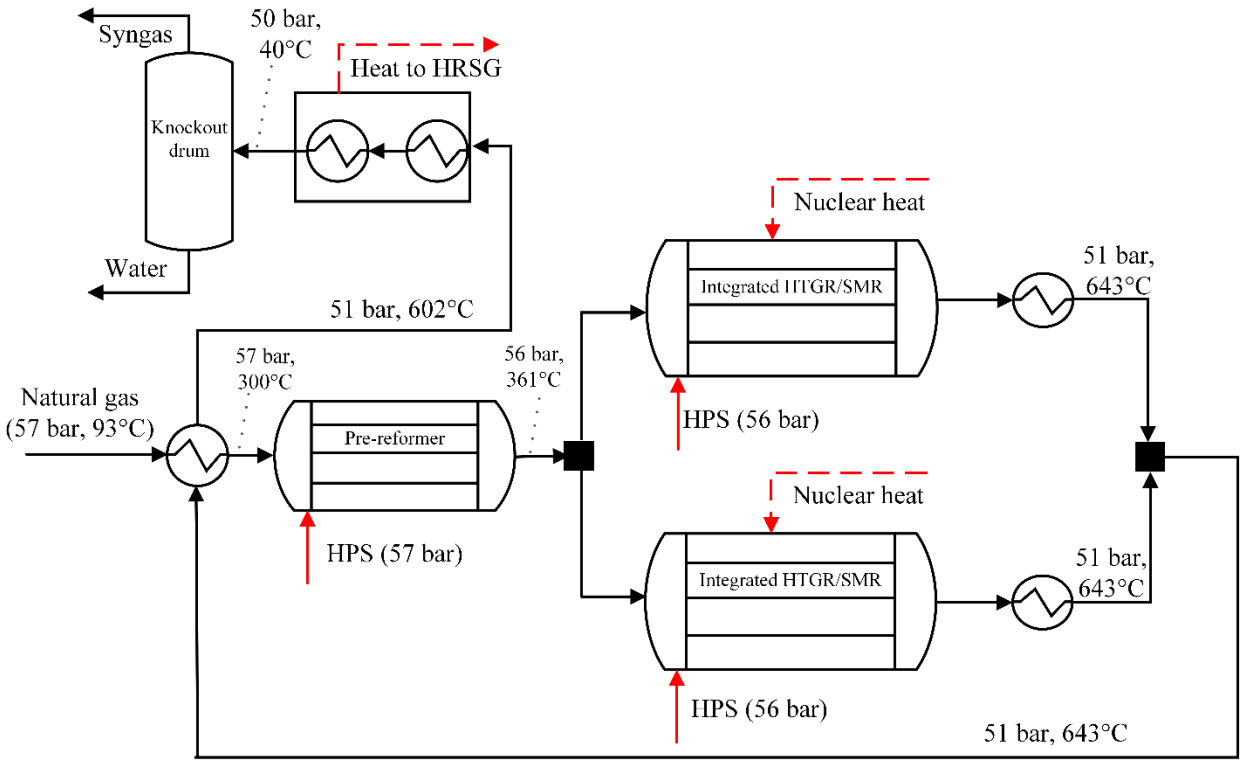

Figure 6. Flowsheet of the integrated HTGR/SMR system in Aspen Plus. HPS = High Pressure Steam.

In the BGTL cases, the CO-rich syngas is mixed with the hydrogen-rich syngas from the integrated RSC/SMR, and shifted syngas from the WGS section to achieve a certain H_2/CO ratio (=2.01) for downstream FT or DME processes. In the BGNTL cases, CO-rich syngas is mixed with H_2 rich syngas from the integrated HTGR/SMR to adjust the H_2/CO ratio. The WGS section is not required in the BGNTL cases since the ratio between biomass and natural gas used in the process can be freely chosen such that the correct H_2/CO ratio in the blended syngas can be obtained.

The mixed syngas then is sent to either FT synthesis to produce gasoline and diesel, DME synthesis. If there is any off-gas in the upstream processes, it is sent to the gas turbine (GT) section to generate electricity. The produced electricity is used for the process needs, and if there is extra electricity it is sold as a product. In the case that produced electricity cannot meet the process needs, it is purchased from the grid.

2.5 Carbon Dioxide Removal

In some of the cases, carbon capture and sequestration is enabled. Depending on the case, a pre-combustion or post-combustion capture process was applied. In the BGTL/FT and BGNTL/FT

processes, CO_2 is captured from the syngas prior to entering the FT synthesis section using an MDEA/piperazine "pre-combustion" process. This is because the CO content in the FT process off-gases is small, CO_2 is more efficiently captured prior to combustion, and little additional CO_2 will be produced during combustion. CO_2/H_2 separation is normally less energy intensive than CO_2/N_2 separation, especially when a large amount of N_2 is present [5]. In addition, the portion of FT off-gases which are recycled are mixed with the fresh syngas feed before entering the CO_2 removal section.

In the BGTL/DME and BGNTL/DME processes, the off-gas of the DME synthesis process still contains a considerable amount of CO which ends as CO_2 in the gas turbine flue gas after combustion. Thus, pre-combustion capture is not a proper option for this case and a post-combustion capture process was applied. Based on the study by Adams et al. [5], an MEA based process is the most efficient and economic choice to capture CO_2 from the gas turbine flue gas.

Both CO_2 capture processes contain an absorption column to separate CO_2 from the syngas mixture, and a stripper column to recover the solvent and separate CO_2. The objective is to capture 90% of CO_2 in the either from syngas or flue gas. The captured CO_2 in this section is sent to the CO_2 compression section to remove water and compress up to 150 bar for sequestration. Both the CO_2 removal processes were based on the models of Adams et al. [25] and the reader is referred to that work for more details.

2.6 Fuel Production Sections

The FT process in the BGTL/FT and BGNTL/FT cases is based on converting syngas with a H_2/CO ratio of 2.01 to hydrocarbons with carbon atom counts from 1 to 60 over a Cobalt based catalyst. The FT reactor outlet is separated into light and heavy hydrocarbons in two flash drums in series. These light and heavy products are sent to a refinery column which was modeled using the PetroFrac block in Aspen Plus to upgrade the products to liquid hydrocarbons which forms diesel and gasoline. The vapor products from the column are sent to an autothermal reformer reactor in the FT unit to produce syngas in a H_2/CO ratio of 2. Depending on the case, this syngas is recycled to the FT reactor or sent back to the CO_2 removal section. The off-gases are sent to the power generation unit (GT). The heavy hydrocarbons from the refinery column are sent to a hydrocracker to break into smaller hydrocarbons using the hydrogen generated in the

pressure-swing absorption column in the FT unit. For brevity we avoid providing detailed information on the FT model and instead refer the reader to Adams et al. [12].

The DME synthesis section was modeled based on the two-step (methanol intermediate) synthesis route model developed by Khojasteh Salkuyeh et al. [30]. In this section, methanol is synthesized using an adiabatic plug flow reactor over a Cu based catalyst. In addition to the methanol synthesis reaction, the water gas shift reaction, the ethanol synthesis reaction, and the methyl formate synthesis reaction are considered simultaneously in the Aspen Plus model of this reactor. The unreacted syngas is then recovered in a flash drum and sent back to the reactor except for a purge stream which is sent to the GT section for power generation. The liquid methanol product is recovered from the mixture in two distillation columns in series. Any off-gases from the distillation are sent to power generation. The distillation columns are modeled using RadFrac in Aspen Plus. The produced purified methanol is then sent to DME production. DME is synthesized in a plug flow reactor over a γ-Alumina catalyst. The liquid product is then distilled (also modeled using a RadFrac block) to recover DME. The unreacted methanol is sent back to the methanol recovery unit and DME product is sent for sale.

2.7 Electricity Production Sections

The GT process, which combusts DME or FT synthesis off-gases, was modeled using an RGibbs block and compressor/ turbine models in Aspen Plus. Off-gases are fed with excess air to the combustion chamber. Some N_2 (from the ASU) is added to the fuel mixture to dilute the fuel and prevent very high temperatures in the combustion chamber [12]. It should be noted that some of the air is split and mixed with the combustion product to decrease the mixture temperature [12, 37].

The waste heat from various sections of the plant is recovered in the HRSG unit to produce steam for plant needs and electricity via steam turbines if extra heat is available. Steam is required in three levels in the plant: low pressure steam (LPS) at 5 bar and 180°C, medium pressure steam (MPS) at 20 bar and 300°C and high pressure steam (HPS) at 50 bar and 500°C. A minimum approach temperature of 10°C is assumed for the various heat exchangers in this unit [38]. This section was modeled in Aspen Plus using the heater, pump, and compressor blocks.

2.8. Cooling Tower

The cooling water required by the system is produced within the plant. The cooling tower was simulated in Aspen Plus using a two-stage equilibrium RadFrac column (with no condenser or reboiler). Air is blown using a fan to cool down the returning cooling water which is at 45°C. During this process some of the water is flees the tower, thus make-up water is added to the tower. This is based on the model of Scott et al. [16] and is described more fully in that work.

2. 9 Plant Sizing, Basis of Comparison, and Optimization

As mentioned previously, the basis of comparison used in this study was that the total thermal input of the feedstocks is 1070 $MW_{HHV.}$ In the BGTL processes, the mass ratio between biomass and natural gas is fixed based on the design requirements of the particular integrated RSC/SMR system which were developed in previous works (e.g. tube arrangements, lengths, wall thicknesses, and diameters; pressure drop; catalyst particle size and loading; material temperature structural limits; safety requirements, etc.), Similarly, in the BGNTL process, the mass ratio between the helium and the natural gas is fixed similarly based on the design requirements of the particular HTGR/SMR system used in this work. Also, in the BGNTL process, the mass ratio between biomass and natural gas is chosen to be the one that yields a syngas blend with the appropriate H_2/CO ratio in the feed to either the FT or DME synthesis process without requiring WGS (or reverse WGS). Thus, the ratios of all feedstocks are determined by process constraints and are not subject to optimization. The final feed rates are shown in Table 2. Note that the nuclear heat input to the BGNTL is nearly identical to the thermal output (103 MW_{th}) of the Peach Bottom I helium-cooled reactor constructed in 1967 [39].

Table 2. Thermal inputs to the plant (HHV basis where applicable).

Plant	Biomass (MWth)	NG feed to SMR (MWth)	Nuclear heat (MW)
BGTL	847.2	223.2	-
BGNTL	478.6	488.3	103.6

Electricity, steam, and cooling water, are produced within the plant boundaries using the waste off-gas and waste heat available (using a combination of the HRSG, GT, and Cooling Tower

sections). In some cases, the available waste energy is not sufficient to meet all electricity and steam needs, and so our analysis assumes that the deficit is purchased from the market for cost purposes. In some cases, there is more waste energy available than can be used, and so this is converted to electricity for sale. All chilled water utility needs are similarly assumed to be purchased from the market.

Although, a formal optimization of the process as a whole was not carried out in this study, the individual sections within the BGNTL and BGTL processes were optimized individually. These section optimizations were either performed in the prior works or performed in the present work using industrial data and best practices. For example, the RSC/SMR design was optimized in a prior work [27] using mathematical programming based on factors such as maximizing methane conversion while meeting certain heat transfer and other constraints. The disadvantage of this approach is that the larger process as a whole was not optimized with an economic objective, but given the very large size of some of the models used for the process, this is not tractable with current computing power. The advantage of this approach is that the resulting processes are likely still sufficiently close to optimality that it is quite suitable for drawing conclusions about the technical and economic feasibility and making value judgements.

3. Results and discussion

3.1 Thermal and Carbon Efficiency

A summary of the simulation results for the BGTL and BGNTL cases are shown in Table 3. In the BGTL case, more biomass feed is introduced to the plant comparing to the BGNTL cases. This is due to the low heating value of biomass which demands more biomass to reform a certain amount of natural gas. In the BGNTL process, a smaller amount of biomass is required to meet the desired H_2/CO ratio due the contribution from nuclear heat.

Table 3. Simulation results.

Case	BGTL/ FT	BGTL/ FT	BGTL/ DME	BGTL/ DME	BGNTL/ FT	BGNTL/ FT	BGNTL /DME	BGNTL /DME
CCS used?	Yes	No	Yes	No	Yes	No	Yes	No
Nuclear heat used?	No	No	No	No	Yes	Yes	Yes	Yes
Energy input (MWe or MW_{HHV})								

Biomass	847.2	847.2	847.2	847.2	478.6	478.6	478.6	478.6
NG	223.2	223.2	223.2	223.2	488.3	488.3	488.3	488.3
Nuclear heat	-	-	-	-	103.6	103.6	103.6	103.6
Extra steam	179.9	89.8	77.6	42.5	132.5	103.2	75.8	63.7
Electricity	133.5	41.8	1.5	-	66.6	2.7	-	-
Energy output (MWe or MW_{HHV})								
Naphtha	172.8	172.9	-	-	167.9	168.1	-	-
Diesel	369.4	369.8	-	-	359.1	359.7	-	-
DME	-	-	489.8	489.8	-	-	546.6	553.9
Electricity	-	-	-	27.0	-	-	38.4	59.2
Thermal efficiency (%)	39.2	45.2	42.6	46.4	41.5	44.9	51.0	54.1
Carbon efficiency (%)	45.1	45.2	36.3	36.3	55.3	55.4	51.1	51.8

The required extra steam and electricity purchases were determined by the simulations and are given in the table. The results show that in three of the four DME production cases (except BGTL/DME with CCS), the plant itself generates more electricity than process needs; however, in the FT cases, some extra electricity must to be purchased from the grid. The reason is that in the FT cases, the available off-gas contains large quantities of CO_2 rather than CO and H_2 and cannot generate the required power. In contrast, in the DME production cases off-gases contain less CO_2 and more CO which can be combusted in the GT and produce more electricity. In the cases with CCS, more electricity is required due to adding CO_2 capture and compression systems. For cost and environmental analysis purposes, it is assumed that the required extra electricity is purchased from the grid in Ontario, Canada. We do not assume that extra electricity is provided by traditional nuclear power (for the BGNTL cases) because the motivating factor for the research is to explore how nuclear energy can be used for non-electricity purposes.

Thermal and carbon efficiencies are employed as indicators to assess the performance of the different plans. The thermal efficiency of a process is defined as the ratio of the sum of all energy outputs divided by all energy inputs on a thermal higher heating value (HHV) basis [14] as given as follows:

$$Thermal\ Efficiency\ (HHV\ based) = \frac{HHV_{Gasoline}+HHV_{Diesel}+HHV_{MeOH}+HHV_{DME}+Power}{HHV_{biomass}+HHV_{NG}+Q_{HTGR}+Q_{Extra}} \quad , \qquad (2)$$

where $Power$ is the electricity output of the system (or 0 if electricity is instead purchased from the grid), Q_{HTGR} is the thermal energy delivered from the nuclear source, and Q_{Extra} is the extra steam or power purchased from the market. For cost and environmental impact purposes, it is assumed that steam is produced from natural gas combustion on an equivalent energy basis.

The carbon efficiency metric uses the definition of [14], which is the carbon atoms in the DME or FT products divided by the carbon atoms in the biomass and natural gas feedstocks. This metric does not consider carbon atoms in any fuels used in the production of steam or electricity purchased from the market, but rather is an indication of the percentage of the feedstock carbon is converted into useful products within the plant boundaries.

The thermal and carbon efficiencies of the different cases are given in Table 3. Comparing the thermal efficiencies indicates that DME production is more efficient than FT liquids production, due to co-producing electricity as another product in the DME cases. Furthermore, the BGNTL/ DME plant is the most efficient since integrated HTGR/SMR process is efficient. However, comparing the carbon efficiencies depicts that FT liquid production better uses primary feedstock carbon, thus resulting in lower direct CO_2 emissions. Of course, since the FT cases require a greater amount of steam and electricity purchases, this may be offset by higher indirect CO_2 emissions depending on the way in which those utilities were made. The carbon efficiency is higher in the nuclear integrated cases, since carbonless nuclear heat displaces biomass or natural gas combustion for the thermal needs of the endothermic SMR reaction.

In our prior study, the efficiency of the BGNTL process in polygenerating FT liquids, MeOH, DME and electricity was studied [23]. Comparing the results of that study with Table 3 indicates that producing one product at a time and using waste off-gases for power production is remarkably more efficient than polygenerating several products.

3.2 Cost Estimation

Raw material, product and utility prices are given in Table S1 in the supplementary material section. All the prices are in Canadian dollars and given in the original year. If the April 2018 price was available for the raw material, product or utility, we used that in the cost analysis. If not, it was updated to 2018 prices using the inflation rate given in Table S3 in the supplementary material section. As shown in the table, high temperature helium is assumed to be a utility which is available in 0.0293 $/kWh (in 2011 dollars). Therefore, the capital cost of purchasing an

HTGR will not be considered in the analysis but is instead incorporated indirectly via treating it as a utility.

To estimate the plant capital cost, equipment cost estimates from the literature were used as given in Table S2 in the supplementary materials. The costs in Table S2 are given for the base size, in the base year, and in US dollars. Thus, they were updated to the considered plant size using the power law rule and updated to 2018 Canadian dollar using the latest Chemical Engineering Plant Cost Index (CEPCI) [40]. The installation cost is assumed to be proportional to the equipment cost. These factors as shown in Table S2 were derived from the literature for different equipment types and taken into account in the cost estimation. The direct cost was approximated as the sum of the equipment and installation costs. Based on Peters et al. [41], the indirect costs were assumed to be 20% of the direct costs and working capital investment was assumed to be 15% of the fixed capital investment. Furthermore, to estimate plant depreciation, the MACRS depreciation tax table was used. The profitability of the studied cases were evaluated by net present value (NPV). The cost data and parameters used to estimate NPV are given in Table S3 in the supplementary material section.

To approximate the capital and operating costs, all the process units shown in Figure 4 and 5 were considered in the cost analysis. The high temperature helium from the HTGR, steam, water, the LO-CAT process and purchased electricity were considered as utility.

The operating cost of the plant was estimated based on the procedure presented by Peters et al. [41] which assumed different components of the operating cost is a function of fixed capital cost, raw material cost or operating labour cost. A summary of these assumptions is given in Table S4 in the supplementary material section.

With these assumptions, the NPV was calculated for each of the studied cases. It should be noted that all the plants were assumed to operate at 85% designed capacity and carbon tax is not considered in the NPV analysis. Instead carbon tax impact on the profitability of the processes is investigated in the sensitivity analysis section. The summary of the cost analysis including the direct costs of each section, fixed capital, revenue from product sales, total production cost and NPV is given in Table 4.

Table 4. Techno-economic analysis results (in 2018 CAD). TPC = Total Product Cost; FCI = Fixed Capital Investment

Case	BGTL/ FT	BGTL/ FT	BGTL/ DME	BGTL/ DME	BGNTL/ FT	BGNTL/ FT	BGNT L/DME	BGNT L/DME
CCS used?	Yes	No	Yes	No	Yes	No	Yes	No
Nuclear heat used?	No	No	No	No	Yes	Yes	Yes	Yes
Direct capital cost of process sections (million $)								
ASU	141	141	120	120	122	122	90	90
Gasifier	182	182	182	182	122	122	122	122
Integrated RSC/SMR	18	18	18	18	-	-	-	-
WGS	21	21	21	21	-	-	-	-
Integrated HTGR/SMR	-	-	-	-	16	16	16	16
CO_2 removal and compression	71	-	74	-	48	-	53	-
FT	217	215	-	-	237	239	-	-
DME	-	-	368	368	-	-	319	333
Compressors	20	18	18	18	21	20	14	14
GT	14	-	55	54	18	19	54	53
HRSG	80	89	76	68	98	114	87	95
Cooling towers	15	1	3	2	4	1	2	2.0
FCI ($M)=1.2×Direct costs	**935**	**822**	**1,121**	**1,021**	**824**	**783**	**909**	**871**
Gasoline sales ($M/yr)	128	128	-	-	124	125	-	-
Diesel sales ($M/yr)	322	322	-	-	313	313	-	-
DME sales ($M/yr)	-	-	487	487	-	-	543	551
Electricity sales ($M/yr)	-	-	-	16	-	-	23	35
Electricity purchase ($M/yr)	79	25	1	-	39	16	-	-
Helium purchase ($M/yr)	-	-	-	-	26	26	26	26
TPC ($M/yr)	**409**	**304**	**425**	**324**	**307**	**272**	**357**	**280**
NPV ($M)	**-1,129**	**-56**	**-686**	**65**	**-228**	**173**	**281**	**697**

In the gasoline & diesel production cases, the FT section is the most expensive section which accounts for 23-30% of the fixed capital investment (FCI) depending on the case. In the DME cases, the DME synthesis section contributes to 32-38% of the fixed capital investment. In all cases, the ASU and gasifier are the two other primary contributors to the capital cost. The fixed capital cost varies from $783 million for BGNTL/FT/woCCS to $1121 million for the BGTL/DME/CCS. The DME cases require 10-24% more capital investment, since the DME synthesis section is more expensive and they require a larger GT unit. The nuclear integrated

cases (BGNTL) needs 5-19% less FCI than the non-nuclear once, since they have a smaller gasifier, ASU, and carbon capture sections. However, this is somewhat misleading since the capital cost of the nuclear reactor is not included in the FCI and instead accounted in the form of an annual utility expense.

Comparing the sales of the different cases indicates sales of diesel and gasoline are almost the same regardless of the process; however, in the DME cases, DME sales are larger in the BGNTL process. This represents higher production rate of DME in the BGNTL cases. The reason is that in the BGNTL process, even though total syngas rate is smaller than the syngas rate in the BGTL, it contains more $CO+H_2$ and less CO_2 than the BGTL process. In the DME cases some electricity is sold as a side product. In contrast, in the FT cases electricity is purchased from the grid. All of these lead a higher profit for the BGNTL/DME process (with and without CCS). The BGNTL/FT process is only profitable without CCS (note that no carbon taxes are considered in Table 4). Based on the economic analysis results, with the current prices of biomass and natural gas BGTL process is not economic and for an investment of $800-900 million, and building BGNTL/DME process is the most profitable option and results in an NPV in the range of $281-697 million.

3.3 Environmental impacts

The environmental impacts of the different cases were assessed by computing the life cycle GHG emissions. In the FT cases with carbon capture and storage, 90% of the CO_2 in the syngas is captured and the CO_2 from the gas turbine is emitted. In the analysis, emissions from the GT is considered as the direct emissions for the FT cases. In the DME cases with carbon capture, 90% of the CO_2 from the flue gas is captured in the MEA process and the rest is emitted to the atmosphere as vent. The vent gas in this case considered as the direct emissions. In the non-CCS cases flue gases of the gas turbine are the direct emissions. If extra steam is required in a process, it is assumed that it is produced using the heat from natural gas combustion on site. The CO_2 emissions from this natural gas combustion is also considered as direct emissions.

Table 5 gives the cradle-to-plant entrance gate emissions in carbon dioxide equivalents (CO_2e) for the natural gas and woody biomass, as well as the plant gate-exit-to-grave CO_2e emissions. The gate-exit-to-grave emissions include the GHG emissions associated with fuel dispensing, distribution, storage, and combustion of the fuels by the end-user. The DME combustion

emissions were approximated assuming the fuel is fully combusted. In addition, we assume that all of the carbon contained in the biomass originated from atmospheric CO_2 [42] and so a credit for CO_2 removal from the atmosphere is assumed based on the carbon content. Net sequestered CO_2 is determined by subtracting the CO_2 feedstock to the biomass gasification process from the total captured CO_2.

Table 5. CO_2e GHG emissions assumptions of the upstream and downstream processes.

Emission source	Value	Reference
Cradle-to-plant entrance gate CO_2e emissions		
Natural gas cradle-to-plant entrance gate CO_2e emissions	7.2 g CO_2e/MJ_{HHV}	[43]
Woody biomass cradle-to-plant-gate emission (including the harvesting and transportation)	0.133 tonne CO_2e / tonne of biomass	[44]
Plant gate-exit-to-grave CO_2e emissions		
Fuel dispensing	138 g CO_2e/GJ	[45]
Fuel distribution and storage	575 g CO_2e/GJ	[45]
Combustion emissions of gasoline	2.35 kg CO_2e/L	[46]
Combustion emissions of diesel	2.68 kg CO_2e/L	[46]
Combustion emissions of DME	1.91 kg CO_2e/kg	Calculated

The detailed GHG emissions accounting of each process are given in Table 6. In the cases that CCS is enabled, net negative GHG emissions are achieved, meaning that even including the combustion of the fuel, there is a net migration from CO_2 in the atmosphere into underground sequestration. Figure 7 compares the cradle-to-grave CO_2e emissions of the different cases with and without CCS. The results show that the DME route has 30-40% less life cycle GHG emissions than FT liquids production when there is no-CCS and significantly lower emissions when CCS is enabled, even when accounting for the lower energy density of DME. Also, BGTL cases have 11-37% larger direct emissions than BGNTL cases and 38-48% larger (negative)

cradle-to-gate entrance emissions due to using more biomass as the feedstock, although the amount of CO_2 that needs to be sequestered is nearly double.

Table 6. Cradle to grave GHG emissions of the plants for 85% capacity.

GHG emission (tCO_2e/yr)	BGTL/ FT	BGTL/ FT	BGTL/ DME	BGTL/ DME	BGNTL/ FT	BGNTL/ FT	BGNTL/ DME	BGNTL/DME
CCS used?	Yes	No	Yes	No	Yes	No	Yes	No
Nuclear heat used?	No	No	No	No	Yes	Yes	Yes	Yes
Direct GHG emissions	287,400	1,234,500	230,340	1,411,900	254,670	892,890	173,790	882,780
Cradle-to-plant-gate-entrance GHG emissions	-1,503,100	-1,518,800	-1,521,000	-1,527,100	-923,300	-785,690	-790,480	-792,580
Net sequestered	-985,740	0	-1,123,060	0	-596,890	0	-664,430	0
Plant-gate-exit-to-grave GHG emissions	1,273,700	1,275,100	724,160	724,160	1,238,000	1,239,300	808,040	818,970
Net Cradle-to-grave GHG emissions	-927,850	1,115,200	-1,689,500	733,300	-27,517	1,416,800	-473,080	979,450
Net Cradle-to-grave GHG emissions (gCO_2e/GJ_{HHV})	-70,610	84,780	-142,319	58,548	-2,155	110,753	-33,368	65,908

Since each DME production process both is more profitable than and has lower GHG emissions than its FT equivalent under the base case market conditions, we compared the life cycle GHG emissions of different cases with standalone NG-to-DME and coal-to-DME processes. The cradle-to-plant gate-exit GHG emissions of a coal-based and natural gas-based DME plants based on the GREET model [47] are 92,700 gCO_2e/GJ_{DME} and 27,310 gCO_2e/GJ_{DME}, respectively. The gate-exit-to-grave emissions of DME are 60,288 gCO_2e/GJ_{DME} from Table 5 results. Thus, the life cycle GHG emissions of coal based and natural gas based DME are 152,988 gCO_2e/GJ_{DME} and 87,598 gCO_2e/GJ_{DME}. These are compared in Figure 8. Based on the results, the BGNTL/DME process without CCS, which is the most efficient and most profitable process among the other studied cases, has GHG emissions that are 57% lower than the traditional coal-to-DME process and 25% lower than the traditional NG-to-DME process.

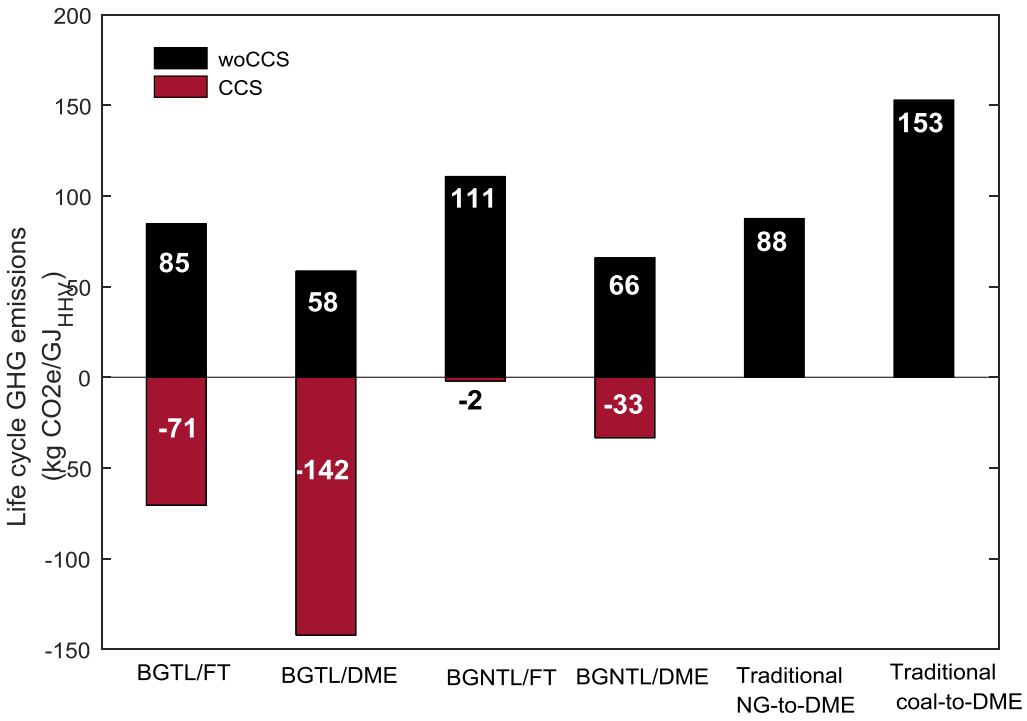

Figure 7. Life cycle GHG emissions of the different cases.

3.4 Sensitivity Analysis

In this section the impact of the uncertain and key parameters on the profitability of the studied systems is considered. The sensitivity analyses were conducted only for the BGNTL/FT/woCCS and BGNTL/DME with or without CCS cases, since the others are not economically promising. The selling price of the fuels (gasoline, diesel and DME), the capital cost of the integrated HTGR/SMR process, the carbon tax, and the wood price are considered as the most uncertain and key parameters in determining the profitability of the systems. Although, the fuel and raw material prices were taken from the most updated sources, they are always subject to change and it is important to analyze the system performance for the possible changes. Furthermore, the capital cost of the integrated reforming systems (HTGR/SMR) is unknown and we assumed that to be the same as a conventional reformer in the HTGR/SMR case, which causes a large uncertainty in the analysis. The carbon tax is also an important factor which strongly influences the inclusion of the CCS system on the studied processes. It should be noted that in the economic analysis in section 3.2, carbon taxes were not included.

The key parameters were perturbed from their base case values as follows: carbon tax was varied between 0 to 100 $/tonne; the integrated HTGR/SMR capital cost was changed from 1 to 7 times its base case value; and the FT liquids, DME ,and wood prices were changed from -20% to +20% of their base case values. The performance of the system under these uncertainties is best demonstrated by the NPV of the different cases. Figure 8 shows the NPV for the different scenarios for each of the studied changes in the parameters. Based on the Figure 8.a., for the considered carbon taxes, non-CCS cases are more profitable than the CCS cases. The BGNTL/DME design without CCS is profitable for carbon taxes smaller than $100 /tonne. Furthermore, it should be noted that with a carbon tax of $50 /tonne all the cases are still profitable. Figure 8.b. shows that even if the integrated reformer price increases by 7 times from its base case value, still all the plants will remain profitable. This implies that NPV of the plants is less sensitive to the integrated reformer capital cost because it is a small portion of the overall process.

Figure 8.c. shows that the NPV of the plants is very sensitive to fuel selling price. Based on this graph, for more than a 10% decrease in the base case diesel and gasoline or DME selling price, both BGNTL/FT and BGNTL/DME designs with CCS become non-economic, however, the BGNTL/DME non-CCS case is still profitable.

Figure 8.d. shows NPV change for a 20% change in the wood purchase price. The results indicate that NPV is less sensitive to this change compared to fuel selling price changes. In this case for a 20% increase in the wood price, all of the plants remain suitable business investments (has a positive NPV).

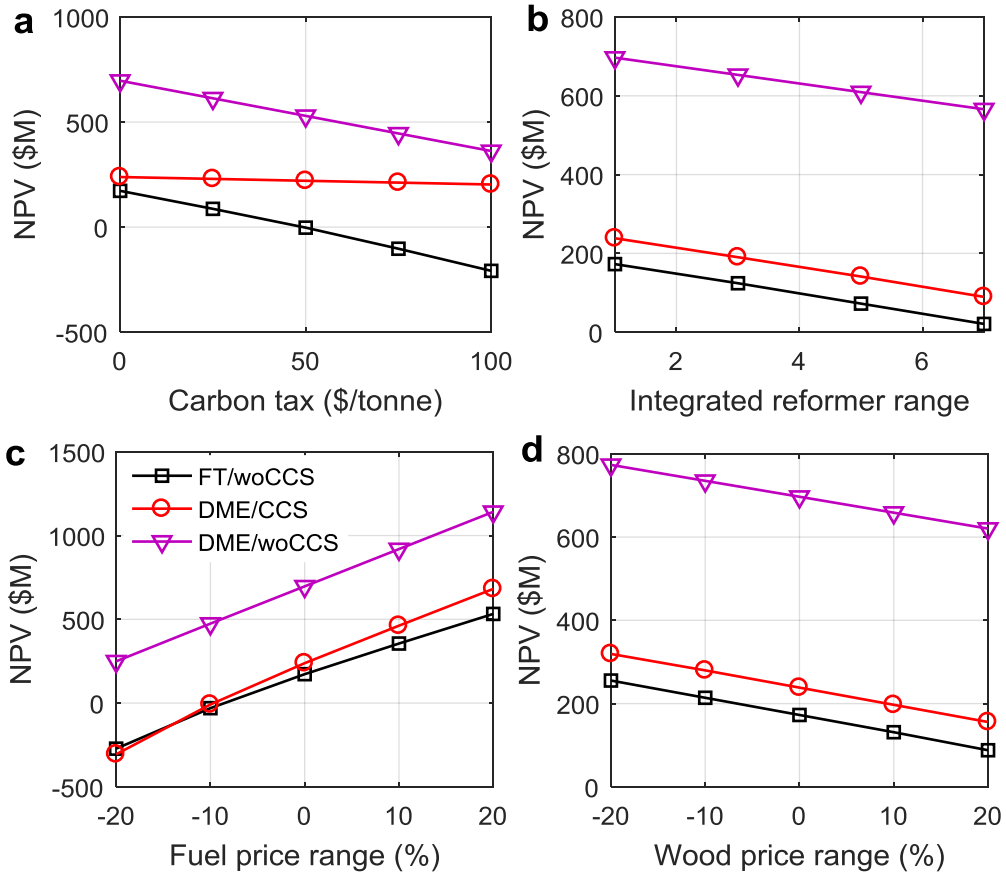

Figure 8. Sensitivity analysis results.

4. Conclusions

A novel combined biomass, gas, and nuclear heat to liquid fuels process was presented for gasoline and diesel or DME production. The BGNTL process was compared against a non-nuclear process of biomass and gas to liquids of the same size to examine nuclear heat integration impact. The key conclusions of the study are listed below:

- The BGNTL process yields high thermal and carbon efficiency. The thermal efficiency can go up to 54 HHV% in the DME production case and carbon efficiency as high as 55% for the FT production case.

- Systems which produce DME result in surplus electricity generation from the off-gases in the plant, thus resulting in a higher thermal efficiency and avoiding the need for importing grid electricity
- With the current prices, the FT liquid production is only profitable if it is produced from the BGNTL process, CCS is not enabled, and there is no carbon tax.
- The most profitable and efficient design, which is the BGNTL/DME, has 57% lower cradle-to-grave GHG emissions than a traditional coal-to-DME plant and 25% lower than a traditional gas-to-DME plant.
- The BGNTL/DME process has 37% lower direct GHG emissions than BGTL/DME when there is no CCS and 25% lower direct emissions when CCS option is enabled.
- All the cases with CCS lead to a negative cradle-to-grave GHG emissions due to using biomass, carbonless heat (in some cases) and a carbon capture system.
- The sensitivity analysis shows that the profitability of the different cases is subject to the current prices and will be affected if market conditions change. Due to the large uncertainty in the fuel and feedstock prices, in the future work it is necessary to conduct an optimization under uncertainty to study the flexibility of the different designs when fluctuation in the market conditions happens.

Acknowledgments

Financial support from the Ontario Ministry of Innovation via Early Researcher Award ER13-09-213 with matching support from the McMaster Advanced Control Consortium is gratefully acknowledged.

Appendix A. Simulation file of the studied designs

The Aspen Plus simulation file of the studied designs can be found in LAPSE (the Living Archive for Process Systems Engineering) with tag LAPSE:2018.0126v1 at the following link:

http://psecommunity.org/LAPSE:2018.0126

Nomenclature

Acronyms

BGNTL	Biomass-gas-nuclear heat-to-liquid
SMR	Steam methane reforming
FT	Fischer-Tropsch
DME	Dimethyl ether
GHG	Greenhouse gas
BGTL	Biomass-gas-to-liquid
CCS	carbon capture and storage
GTL	Gas-to-liquids process
MHR	Modular helium reactor
CGNTL	Coal-gas-and-nuclear-to-liquids
CTL	Coal-to-liquids
CGTL	Coal-and-gas-to-liquids
MeOH	Methanol
HTGR	High temperature gas-cooled reactor
RSC	Radiant syngas cooler
HHV	High heating value
LHV	Low heating value
WGS	Water gas shift
LHS	Latin hypercube sampling
GT	Gas turbine
ASU	Air separation unit
LPS	Low pressure steam
MPS	Medium pressure steam
HPS	High pressure steam
NG	Natural gas
MDEA	Methyl di-ethanolamine
CEPCI	Chemical Engineering Plant Cost Index
NPV	Net present value

FIC	Fixed capital investment
TPC	Total product cost

References

[1] Baliban RC, Elia JA, Floudas CA. Novel natural gas to liquids processes: Process synthesis and global optimization strategies. AIChE J 2013; 59:505-31.

[2] Liu G, Yan B, Chen G. Technical review on jet fuel production. Renew Sustain Energy Rev 2013;25:59–70.

[3] Mantripragada HC, Rubin ES. CO_2 reduction potential of coal-to-liquids (CTL) process: effect of gasification technology. Enrgy Proced 2011;4:2700–7.

[4] Jaramillo P, Griffin WM, Matthews HC. Comparative analysis of the production costs and life-cycle GHG emissions of FT liquid fuels from coal and natural gas. Environ Sci Tech 2008;42:7559-65.

[5] Adams TA II, Hoseinzade L, Madabhushi, PB and Okeke IJ. Comparison of CO_2 capture approaches for fossil-Based power generation: review and meta-study. Processes 2017; 5(3): 44.

[6] Zhang X, Li S, Jin H. A polygeneration system based on multiinput chemical looping combustion. Energies 2014; 7:7166-77.

[7] Khojasteh Salkuyeh Y, Adams TA II. Co-production of olefins, fuels, and electricity from conventional pipeline gas and shale gas with near-zero CO_2 emissions. Part I: Process development and technical performance. Energies 2015; 8:3739-61.

[8] Serra LM, Lozano MA, Ramos J, Ensinas AV, and Nebra SA. Polygeneration and efficient use of natural resources. Energy 2009; 34(5):575-86.

[9]Adams TA II, Ghouse JH. Polygeneration of fuels and chemicals. Curr Opin Chem Eng 2015;10:87-93.

[10] Jana K, Ray A, Majoumerd MM, Assadi M, De S. Polygeneration as a future sustainable energy solution–A comprehensive review. Appl Energy 2017;202:88-111.

[11] Kieffer M, Brown T, Brown RC. Flex fuel polygeneration: Integrating renewable natural gas into Fischer–Tropsch synthesis. Appl Energy 2016;170:208-18.

[12] Adams TA II, Barton PI. Combining coal gasification and natural gas reforming for efficient polygeneration. Fuel Process Technol 2011;92:639-55.

[13] Adams TA II, Barton PI. Combining coal gasification, natural gas reforming, and solid oxide fuel cells for efficient polygeneration with CO_2 capture and sequestration. Fuel Process Technol 2011;92:2105-15.

[14] Khojasteh Salkuyeh Y, Adams TA II. Combining coal gasification, natural gas reforming, and external carbonless heat for efficient production of gasoline and diesel with CO_2 capture and sequestration. Energ Convers Manage 2013;74:492-504.

[15] Government of Ontario. Ontario's Five Year Climate Change Action Plan 2016-2020 (p86). http://www.applications.ene.gov.on.ca/ccap/products/CCAP_ENGLISH.pdf

[Accessed Aug 2017].

[16] Scott JA, Adams TA II. Biomass-gas-and-nuclear-to-liquids (BGNTL) processes Part I: model development and simulation. Canadian J Chem Eng 2018; in press, CJCE-18-0053.R2.

[17] Yan XL, Hino R. Nuclear hydrogen production handbook. CRC Press; 2011.

[18] Fedders H, Harth R, Höhlein B. Experiments for combining nuclear heat with the methane steam-reforming process. Nucl Eng Des 1975;34(1):119-27.

[19] Höhlein B, Niessen H, Range J, Schiebahn HJ, Vorwerk M. Methane from synthesis gas and operation of high-temperature methanation. Nucl Eng Des 1984;78(2):241-50.

[20] Inagaki Y, Nishihara T, Takeda T, Hada K, Ogawa M, Shiozawa S, Miyamoto Y. Development programme on hydrogen production in HTTR. No. IAEA-TECDOC--1210 2001.

[21] Hoseinzade L, Adams TA II. Modeling and simulation of an integrated steam reforming and nuclear heat system. Int J Hydrogen Energy 2017;42(39): 25048-62.

[22] Hoseinzade L, Adams TA II. Dynamic modeling of integrated mixed reforming and carbonless heat systems. Ind Eng Chem Res 2018;57:6013-23.

[23] Hoseinzade L, Adams TA II. Combining biomass, natural gas, and carbonless heat to produce liquid fuels and electricity. Comput Aided Chem Eng 2018;43:1401-06.

[24] Adams TA II, Barton PI. High-efficiency power production from coal with carbon capture. AIChE J 2010;56:3120-36.

[25] Adams TA II, Khojasteh Salkuyeh Y, Nease J. Processes and simulations for solvent-based CO_2 capture and syngas cleanup. In: reactor and process design in sustainable energy technology, ed: Fan Shi. Elsevier: Amsterdam. ISBN 978-0-444-59566-9, 2014.

[26] Ghouse JH, Seepersad D, Adams TA II. Modelling, simulation and design of an integrated radiant syngas cooler and steam methane reformer for use with coal gasification, Fuel Process Technol 2015;138:378-89.

[27] Ghouse JH, Adams TA II. Optimal design of an integrated radiant syngas cooler and steam methane reformer using NLP and meta-heuristic algorithms. Comput Aided Chem Eng 2016;38:1431-36.

[28] Adams TA II, Barton PI. High-efficiency power production from coal with carbon capture. AIChE J 2010;56:3120-36.

[29] Adams TA II, Barton PI. A dynamic two-dimensional heterogeneous model for water gas shift reactors. Int J Hydrogen Energy 2009;34:8877-91.

[30] Khojasteh Salkuyeh Y, Adams TA II. A new power, methanol, and DME polygeneration process using integrated chemical looping systems. Energ Convers Manage 2014;88:411-25.

[31] Zhang L, Ninomiya Y, Wang Q, Yamashita T. Influence of woody biomass (cedar chip) addition on the emissions of PM10 from pulversied coal combustion. Fuel 2011;90:77-86.

[32] Hewson D, Oo A, Albion KJ, Keir A. Biomass residuals study for OPG repowering program. Report of the University of Western Ontario Research & Development Park, Sarnia-Lambton Campus; 2011,

http://www.canadiancleanpowercoalition.com/pdf/BM22%20-%20Biomass%20Residuals%20Study%20for%20OPG%20Repowering%20Program.pdf

[33] Van der Drift A, Boerrigter A, Coda H, Cieplik B, Hemmes MK, Van Ree K, Veringa HJ. Entrained flow gasification of biomass. Report ECN-C--04-0.39 of Energieonderzoek Centrum Nederland, Revision A; April 2004. Accessible at

https://www.ecn.nl/docs/library/report/2004/c04039.pdf

[34] Field RP, Brasington R. Baseline flowsheet model for IGCC with carbon capture. Ind Eng Chem Res 2011;50:11306-12.

[35] Feedstock EW. Equipment design and cost estimation for small modular biomass systems, synthesis gas cleanup, and oxygen separation equipment. Nat Renew Energy Lab 2006.

[36] Okoli C, Adams TA II. Design and economic analysis of a thermochemical lignocellulosic biomass-to-butanol process. Ind Eng Chem Res 2014;53:11427-41.

[37] Clausen LR, Elmegaard B, Houbak N. Technoeconomic analysis of a low CO_2 emission dimethyl ether (DME) plant based on gasification of torrefied biomass. Energy 2010;35:4831-42.

[38] Seider WD, Seader JD, Lewin DR, Widago S. Product and process design principles: synthesis, analysis and design.3rd ed. Hoboken, NJ: Wiley; 2008.

[39] LaBar MP, Shenoy AS, Simon WA, Campbell EM, Hassan YA. The gas-turbine modular helium reactor in: nuclear energy materials and reactors – Vol. II, Hassan YA and Chaplin RA, eds. EOLSS Publications; 2010.

[40] Chemical engineering cost index, 2017.

[41] Peters M S, Timmerhaus K D. Plant design and economics for chemical engineers. 4th ed. New York: McGraw-Hill; 1991.

[42] Jiang Y, Bhattacharyya D. Process modeling of direct coal-biomass to liquids (CBTL) plants with shale gas utilization and CO_2 capture and storage (CCS). Appl Energy 2016;183:1616-32.

[43] ICF Consulting Canada. Life Cycle Greenhouse Gas Emissions of Natural Gas, A LITERATURE REVIEW OF KEY STUDIES COMPARING EMISSIONS FROM NATURAL GAS AND COAL. The Canadian Natural Gas Initiative (CNGI); 2012,

http://www.capp.ca/~/media/capp/customer-portal/documents/215278.pdf

[44] Zhang Y, McKechnie J, Cormier D, Lyng R, Mabee W, Ogino A, Maclean HL. Life cycle emissions and cost of producing electricity from coal, natural gas, and wood pellets in Ontario, Canada. Environ Sci Technol 2010; 44:538–44.

[45] S&T Consultants Inc. The addition of Bio-Butanol to GHGenius and a review of the GHG Emissions from Diesel Engines With Urea SCR; 2007,

http://www.ghgenius.ca/reports/ButanolGHGenius.pdf

[46] How much carbon dioxide is produced by burning gasoline and diesel fuel? - FAQ - U.S. Energy Information Administration (EIA),

http://www.eia.gov/tools/faqs/faq.cfm?id=307&t=11

[Accessed 6 May 2016].

[47] GREET. U-Chicago Argonne LLC, Argonne, USA 2017.

[48] Natural Gas Rate Updates. (n.d.),

http://www.ontarioenergyboard.ca/OEB/Consumers/Natural+Gas/Natural+Gas+Rates /

[Accessed 30 Jan 2018].

[49] Government of Canada, N. R. C. (n.d.-a). Average Gasoline Retail Prices in Canada,

http://www2.nrcan.gc.ca/eneene/sources/pripri/prices_bycity_e.cfm

[Accessed 30 Jan, 2018].

[50] Dimethyl Ether Prices - Alibaba.com. (n.d.),

https://www.alibaba.com/showroom/dimethyl-ether-prices.html

[Accessed 30 Jan, 2018].

[51] Ontario electricity pricing,

http://www.ieso.ca/en/learn/electricity-pricing/for-residents-and-small-businesses

[Accessed 30 Jan, 2018].

[52] Perales AV, Valle CR, Ollero P, Gómez-Barea A. Technoeconomic assessment of ethanol production via thermochemical conversion of biomass by entrained flow gasification. Energy 2011;36(7):4097-4108.

[53] Hamelinck CN, Faaij AP, den Uil H, Boerrigter H. Production of FT transportation fuels from biomass; technical options, process analysis and optimisation, and development potential. Energy 2004;29(11):1743-71.

[54] Larson ED, Tingjin R. Synthetic fuel production by indirect coal liquefaction. Energy Sustain Dev 2003;7(4):79-102.

[55] Larson ED, Jin H, Celik FE. Gasification-based fuels and electricity production from biomass, without and with carbon capture and storage. Princeton Environmental Institute, Princeton University; 2005.

[56] Kreutz TG, Larson ED, Liu G, Williams RH. Fischer-Tropsch fuels from coal and biomass. In 25th annual international Pittsburgh coal conference. Princeton University Pittsburg; 2008.

[57] Hoseinzade L, Adams TA II. Supply chain optimization of flare-gas-to-butanol processes in Alberta. Canadian J Chem Eng 2016;94:2336-54.

[58] Historic inflation Canada – historic CPI inflation Canada. (n.d.).,

http://www.inflation.eu/inflation-rates/canada/historic-inflation/cpi-inflation-canada.aspx

[Accessed 30 Jan, 2018].

[59] Government of Canada, C. R. A. Corporation tax rates,

http://www.cra-arc.gc.ca/tx/bsnss/tpcs/crprtns/rts-eng.html

[Accessed 30 Jan, 2018].

e-component

Click here to download e-component: SupplementaryMaterials.docx